

## Impact of Pulmonary Hemodynamics and Ventricular Interdependence on Left Ventricular Diastolic Function in Children With Pulmonary Hypertension

Dale A. Burkett, MD; Cameron Slorach, RDCS; Sonali S. Patel, MD, PhD;  
Andrew N. Redington, MBBS, MD; D. Dunbar Ivy, MD; Luc Mertens, MD, PhD;  
Adel K. Younoszai, MD; Mark K. Friedberg, MD

**Background**—Through ventricular interdependence, pulmonary hypertension (PH) induces left ventricular (LV) dysfunction. We hypothesized that pediatric PH patients have LV diastolic dysfunction, related to adverse pulmonary hemodynamics, leftward septal shift, and prolonged right ventricular systole.

**Methods and Results**—Echocardiography was prospectively performed at 2 institutions in 54 pediatric PH patients during cardiac catheterization and in 54 matched controls. Diastolic LV measures including myocardial deformation were assessed by echocardiography. PH patients had evidence of LV diastolic dysfunction, most consistent with impaired LV relaxation, though some features of reduced ventricular compliance were present. PH patients demonstrated the following: reduced mitral  $E$  velocity and inflow duration, mitral  $E'$  and  $E'/A'$ , septal  $E'$  and  $A'$ , pulmonary vein  $S$  and  $D$  wave velocities, and LV basal global early diastolic circumferential strain rate and increased mitral  $E$  deceleration time, LV isovolumic relaxation time, mitral  $E/E'$ , and pulmonary vein  $A$  wave duration. PH patients demonstrated leftward septal shift and prolonged right ventricular systole, both known to affect LV diastole. These changes were exacerbated in severe PH. There were no statistically significant differences in diastolic measures between patients with and without a shunt and minimal differences between patients with and without congenital heart disease. Multiple echocardiographic LV diastolic parameters demonstrated weak-to-moderate correlations with invasively determined PH severity, leftward septal shift, and prolonged right ventricular systole.

**Conclusions**—Pediatric PH patients exhibit LV diastolic dysfunction most consistent with impaired relaxation and reduced myocardial deformation, related to invasive hemodynamics, leftward septal shift, and prolonged right ventricular systole. (*Circ Cardiovasc Imaging*. 2016;9:e004612. DOI: 10.1161/CIRCIMAGING.116.004612.)

**Key Words:** cardiac catheterization ■ diastole ■ echocardiography ■ hypertension, pulmonary ■ pediatrics

Pulmonary hypertension (PH) is a progressive disease with substantial mortality.<sup>1,2</sup> Although right ventricular (RV) systolic dysfunction is a central cause of morbidity and death in PH,<sup>1-4</sup> through ventricular interdependence, the left ventricle (LV) is significantly impacted. LV systolic dysfunction has been highlighted as a key risk factor for adverse outcomes in adult PH.<sup>5</sup> Moreover, we recently documented impaired LV systolic mechanics in pediatric PH.<sup>6</sup> However, LV diastolic function, an important component of cardiac (dys)function, remains underinvestigated in PH and is consequently not accounted for in its management.

### See Editorial by Hansmann See Clinical Perspective

Increased RV pressure and systolic duration can cause leftward septal shift during LV relaxation, potentially affecting LV

diastole. Adult PH studies reveal decreased LV filling rates and size and abnormal pulmonary vein and mitral valve flow patterns.<sup>5,7-14</sup> However, the hemodynamic impact of PH on LV diastolic function (including myocardial performance) has not been fully evaluated as few studies have directly related the 2; fewer yet have done so simultaneously. Furthermore, little is known about how congenital heart disease (CHD) and intra/extracardiac shunting—commonly associated with pediatric PH—affect cardiopulmonary hemodynamics and LV diastolic function in PH.

Accordingly, this study aimed to investigate LV diastolic function in pediatric PH and the relation to invasive pulmonary hemodynamics, using simultaneous echocardiography and cardiac catheterization. We hypothesized that children and young adults with PH have LV diastolic dysfunction, related to adverse pulmonary hemodynamics, leftward septal shift, and prolonged RV systole.

Received January 29, 2016; accepted August 8, 2016.

From the Division of Cardiology, Heart Institute, Children's Hospital Colorado, University of Colorado, Aurora (D.A.B., S.S.P., D.D.I., A.K.Y.); and Division of Cardiology, The Labatt Family Heart Center, Hospital for Sick Children, University of Toronto, Ontario, Canada (C.S., A.N.R., L.M., M.K.F.). Correspondence to Dale A. Burkett, MD, Division of Cardiology, Children's Hospital Colorado, 13123 E 16th Ave, B-100, Aurora, CO 80045. E-mail dale.burkett@childrenscolorado.org

© 2016 American Heart Association, Inc.

*Circ Cardiovasc Imaging* is available at <http://circimaging.ahajournals.org>

DOI: 10.1161/CIRCIMAGING.116.004612

## Methods

### Study Population

Between November 1, 2008, and October 1, 2013, at Children's Hospital Colorado and the Hospital for Sick Children (SickKids) in Toronto, we prospectively performed simultaneous transthoracic echocardiography in children and adolescents during clinically indicated right-heart catheterization for initial evaluation of suspected PH or routine follow-up of previously documented precapillary PH (resting mean pulmonary artery pressure  $\geq 25$  mmHg and pulmonary capillary wedge pressure [PCWP]  $\leq 15$  mmHg at catheterization).<sup>15</sup> We previously published systolic strain results in this patient cohort.<sup>6</sup> The study was approved by the Institutional Review Boards at both institutions. Informed consent was obtained for all patients.

We excluded those with conditions that might directly impact LV function aside from PH, including single ventricle physiology, active pacing, cardiomyopathies, heart transplant, (branch) pulmonary artery stenosis, uncontrolled systemic hypertension, ventricular septal defect occlusion devices, any left-sided obstructive lesion, PCWP  $>15$  mmHg, or lack of raw echocardiography data preventing analysis. Ten patients were excluded, leaving 54 in our final cohort (37 from Children's Hospital Colorado and 17 from SickKids); 1 patient was found not to have PH on initial diagnostic catheterization and thus was excluded from comparisons of PH patients versus controls but included in correlative data.

### Right-Heart Catheterization

Under general anesthesia, a right-heart catheterization was performed by individuals blinded to echocardiographic measures. Cardiac index was measured by thermodilution (if no shunting) or calculated using the modified Fick equation (if shunt present); pulmonary (Qp) blood flow and systemic (Qs) blood flow were documented. We measured pressures in the right atrium, RV, pulmonary artery, left atrium (PCWP used when left atrium not accessed), and femoral (systemic) artery. We calculated the transpulmonary gradient (PCWP served as a surrogate when left atrial pressure not obtained) and systemic and indexed pulmonary vascular resistances (PVRi).

### Echocardiography

During the baseline condition of cardiac catheterization, we used transthoracic echocardiography to obtain images from apical 4- and 2-chamber views and parasternal short-axis views at the LV base (mitral valve), mid (papillary muscles), and apex (apical to the papillary muscles), using a General Electric (GE) Vivid 7 or E9 system (GE Healthcare). Results of 3 to 5 cardiac cycles were averaged to account for beat-to-beat variability. Measurements were made by individuals blinded to clinical and catheterization data (not present during cardiac catheterization).

Simpson's biplane LV volumes and ejection fraction were calculated.<sup>16</sup> LV eccentricity index was calculated from mid parasternal short-axis images at end-diastole and end-systole (Figure 1).<sup>17</sup>

From the apical 4-chamber view, we recorded the following: pulmonary vein systolic (S), diastolic (D), and atrial contraction flow-reversal (A) wave velocities and A wave duration; mitral and tricuspid peak early (E) and late (A) diastolic velocities; mitral E deceleration time; mitral inflow duration (mitral valve opening to closure); and duration of aortic valve ejection.

To assess whether RV systole is prolonged beyond LV systole, and the potential impact on LV filling, the time from QRS onset to initiation of tricuspid and mitral valve inflow (Figure 2) was recorded (heart rates within 5 bpm). This surrogate measure of ventricular systolic duration includes isovolumic relaxation time—a period where RV pressure can still be elevated compared with LV pressure. The ratio of time to tricuspid inflow (RV systole) divided by time to mitral inflow (LV systole) quantified RV systolic prolongation: a value of 1=simultaneous completion of RV and LV systole and  $>1$ =prolonged RV systole.

From the apical 4-chamber view, pulsed-wave tissue Doppler imaging was performed at the lateral and septal mitral annulus and the lateral tricuspid annulus; peak early (E') and late (A') diastolic myocardial annular velocities and isovolumic relaxation time (by tissue Doppler imaging of the lateral mitral annulus) were recorded.

### Speckle-Tracking Echocardiography

Two-dimensional images were used for off-line speckle-tracking echocardiography analysis (EchoPAC version 113; GE Healthcare).

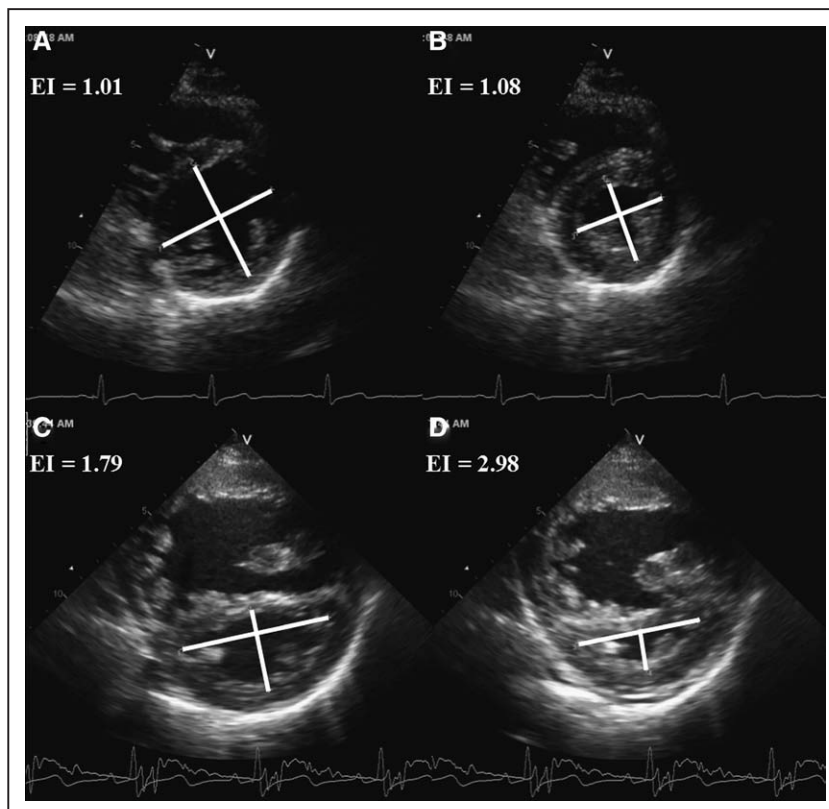


**Figure 1.** Normal septal geometry in a control patient is quantified with end-diastolic (A) and end-systolic (B) eccentricity index (EI). Leftward septal shift in a pulmonary hypertension patient quantified with end-diastolic (C) and end-systolic (D) EI.

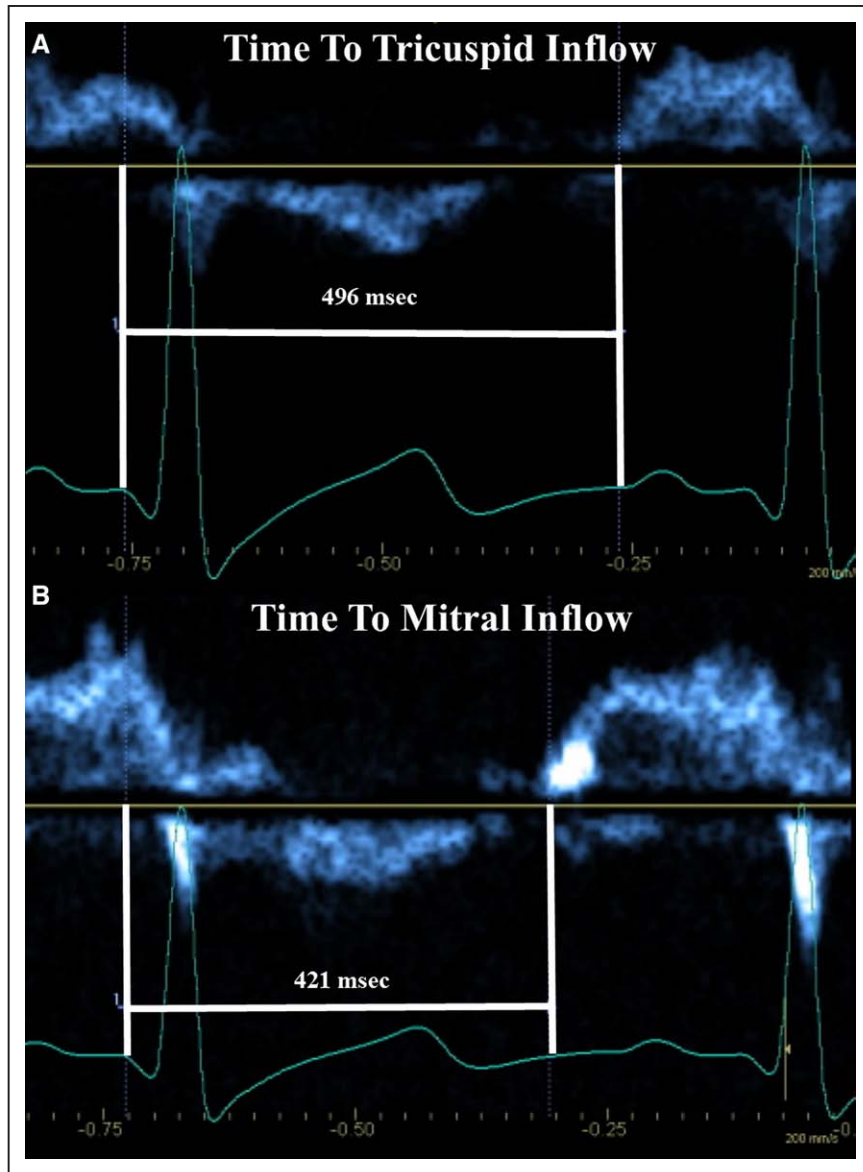


**Figure 2.** Timing from onset of QRS to the onset of tricuspid (A) and mitral (B) inflow, as a surrogate measure of right (A) and left (B) ventricular systole. The ratio of right ventricular systolic duration divided by left ventricular systolic duration yields a quantifiable measure of the degree of prolongation of right ventricular systole. Here, the ratio measures 1.18.

The region of interest was set to myocardial wall thickness. Tracking was visually assessed throughout the cardiac cycle, and the region of interest adjusted as needed to ensure accurate tracking.<sup>18</sup> If  $\geq 4$  segments tracked well by visual and EchoPAC assessment, the curve was accepted; segments that tracked poorly were excluded. Aortic valve closure, by pulsed-wave Doppler (heart rate within 5 bpm to images used for strain), defined LV end-systole. LV (IVS included as part of the LV) peak global early diastolic longitudinal strain rate (DLSR) was assessed from the apical 4-chamber view. LV peak global early diastolic circumferential strain rate (DCSR) was assessed from the base, mid, and apical parasternal short-axis views.

Peak diastolic apical and basal rotation rates (recoil) were re-recorded to determine peak diastolic untwist rate (apical recoil–basal recoil), which was indexed to LV length.

### Control Population

Comparable measurements were obtained from the echocardiograms of 54 age-, sex-, and institution-matched healthy children (37 at Children's Hospital Colorado and 17 at SickKids); no controls underwent catheterization. Subjects were healthy volunteers or children undergoing evaluation for murmur, chest pain, palpitations, syncope, or family history of CHD, with a normal echocardiogram.<sup>15</sup> We excluded those with documented arrhythmias, chemotherapy exposure,

family history of cardiomyopathy or bicuspid aortic valve,<sup>19</sup> systemic illness, or documented/suspected genetic abnormality. The systolic strain values of this control cohort was previously published.<sup>6</sup>

### Statistical Analysis

Data were not normally distributed by the Shapiro–Wilk test. Thus, continuous data are presented as median with interquartile range unless otherwise noted; categorical data are presented as frequencies (%). Comparative analysis was performed using Wilcoxon, Mann–Whitney, and  $\chi^2$  testing as appropriate. Matched data were analyzed for differences using Wilcoxon signed-rank testing. Exact methods were used as necessary. ANOVA testing was used to define the presence of differences between subgroups; post hoc analysis was performed with Student–Newman–Keuls test. Spearman correlation coefficients were used to assess relationships between echocardiographic LV filling parameters, invasive hemodynamics, septal shift, and prolonged RV systole. Reproducibility was assessed for diastolic strain measures. To assess interobserver variability, SickKids PH echocardiograms (31.5% of patients with PH) were reanalyzed by a second observer (C.S.), also blinded to clinical and catheterization data. To assess intraobserver variability, 10% of echocardiograms were reanalyzed at least 8 weeks apart. Inter-rater and intrarater reliability were calculated using intraclass correlation coefficients with

95% confidence interval. A  $P$  value of  $<0.05$  was considered statistically significant. All analyses were performed using SAS software, version 9.3 (SAS Corporation, Cary, NC).

## Results

### Patient Characteristics

Patient characteristics are presented in Table 1 and hemodynamic data in Table 2. In total, 54 PH patients and 54 controls were analyzed. One study patient did not have PH on initial catheterization; he and his matched control were omitted from comparisons between PH and controls. Most PH patients were women (34/53, 64.2%), and born with CHD (33/53, 62.3%), defined as any structural defect (including a patent foramen ovale); some with CHD had multiple defects (7/33, 21.2%). Common abnormalities were atrial and ventricular septation defects and a patent ductus arteriosus; other forms of CHD included atrioventricular septal defect (2), transposition of the great arteries (1), and anomalous pulmonary venous drainage because of a posterior/leftward deviated atrial septum, repaired without pulmonary vein manipulation/obstruction (2).

Of those born with CHD, 36.4% (12/33) underwent previous repair. Thus, 63.6% (21/33) of those with CHD, and 39.6% (21/53) of the entire PH cohort, had a potential intra/extracardiac shunt at the time of catheterization; this group had a median pulmonary-to-systemic blood flow ratio ( $Q_p:Q_s$ ) of 1.16 (1.00–1.55). Cardiac index was preserved across the entire PH cohort and did not correlate with mean pulmonary artery pressure ( $r=0.06$ ;  $P=0.67$ ) or PVRi ( $r=-0.27$ ;  $P=0.07$ ). All patients had systemic saturations  $>90\%$ .

Idiopathic PH was present in 26.4% of patients (14/53). Other causes included CHD, lung disease/hypoxia, hematologic

disorders, chronic thromboembolism, or a combination of causes. Sixteen patients had  $\geq 1$  PH-related hospital admission (24 admissions total). There was 1 death and 1 transplant (lung) during the study period.

### Echocardiographic Measures

LV echocardiographic measures are presented in Table 3. LV eccentricity indices were increased in PH, consistent with increased leftward septal shift. Indexed end-systolic volume was larger in PH patients, even after controlling for shunting. Although at the lower limits of normal, LV ejection fraction was significantly lower in PH compared with controls.

### LV Diastolic Measures

Patients with PH demonstrated the following: reduced pulmonary venous S and D velocities and increased A wave duration, reduced mitral  $E$  and inflow duration and increased  $E$  deceleration time, reduced  $E'$  in the septum and free-wall and  $A'$  in the septum, increased mitral  $E/E'$ , increased isovolumic relaxation time, and decreased basal DCSR and a trend toward reduced LV DLSR and mid DCSR. Apical recoil was increased (more negative) in PH, resulting in increased indexed diastolic untwist rate, despite no statistically significant difference in basal recoil. RV systole was prolonged.

### Severe PH

To further assess the impact of pulmonary hemodynamics on LV diastolic function, PH patients were separated into quartiles of severity, determined by the ratio of pulmonary-to-systemic mean arterial pressures (MPAP/MAP). Although cardiac index was not significantly different statistically between quartiles ( $P=0.59$ ), median MPAP/MAP and PVRi for the most severe quartile were higher than each of the other

**Table 1. Patient Characteristics**

	PH Patients (n=53)	Control Subjects (n=53)	$P$ Value
Age, y (range)	8 (0–23)	8 (0–23)	0.99
Female sex	34 (64.2)	34 (64.2)	1.00
Weight, kg	32.5 (14.7–51.4)	30.6 (16.3–54.8)	0.20
Height, cm	133.0 (98.0–161.0)	136.0 (104.5–162.0)	0.11
Body surface area, m <sup>2</sup>	1.12 (0.63–1.52)	1.10 (0.69–1.57)	0.06
Heart rate, bpm	81 (70–100)	79 (65–93)	0.09
Congenital heart disease	33 (62.3)	...	...
Atrial septal defect/patent foramen ovale	24 (45.3)	...	...
Ventricular septal defect	5 (9.4)	...	...
Patent ductus arteriosus	11 (20.8)	...	...
Other	5 (9.4)	...	...
Shunt present at catheterization	21 (39.6)	...	...
Idiopathic pulmonary arterial hypertension	14 (26.4)	...	...
World Health Organization Class			
Not available	15 (28.3)	...	...
I/II	15 (28.3)/16 (30.2)	...	...
III/IV	6 (11.3)/1 (1.9)	...	...

Data are presented as n (%) or median (interquartile range), unless otherwise noted. PH indicates pulmonary hypertension.

**Table 2. Hemodynamic Characteristics**

	PH Patients (n=53)	Severe PH (n=13)	CHD (n=33)	No CHD (n=20)	CHD <i>P</i> Value	Shunt (n=21)	No Shunt (n=32)	Shunt <i>P</i> Value
MPAP, mmHg	33.0 (25.0–43.0)	60.0 (46.0–61.0)	40.5 (28.0–52.0)	27.0 (23.0–31.0)	0.0074*	41.5 (32.0–54.0)	28.5 (20.5–38.5)	0.0082*
MAP, mmHg	58.0 (55.0–63.0)	58.0 (52.0–60.0)	59.0 (53.0–63.0)	57.0 (55.0–63.0)	0.77	57.5 (52.5–61.0)	59.5 (55.0–63.0)	0.26
MPAP/MAP	0.59 (0.43–0.79)	1.00 (0.81–1.04)	0.66 (0.42–0.94)	0.44 (0.39–0.56)	0.0086*	0.71 (0.59–0.97)	0.46 (0.35–0.61)	0.003*
SPAP, mmHg	52.0 (38.0–63.0)	84.0 (63.0–90.0)	58.0 (39.0–67.0)	41.0 (35.0–52.0)	0.0134*	60.5 (52.0–73.0)	43.0 (34.0–56.0)	0.0068*
DPAP, mmHg	23.0 (15.0–32.0)	42.0 (33.0–46.0)	27.0 (14.0–35.0)	19.0 (15.0–22.0)	0.035*	29.5 (22.0–36.0)	19.5 (14.0–27.0)	0.0186*
TPG, mmHg	23.0 (16.0–35.0)	51.0 (38.0–54.0)	30.0 (19.0–43.0)	17.0 (15.0–22.0)	0.0029*	33.0 (22.0–48.0)	18.5 (13.5–29.0)	0.0035*
DTPG, mmHg	13.0 (6.0–26.0)	35.0 (26.0–39.0)	16.5 (5.0–27.0)	10.0 (6.0–12.0)	0.0087*	21.5 (13.0–28.0)	11.0 (5.0–16.0)	0.0069*
MLAP, mmHg	8.5 (7.0–10.0)	7.0 (6.0–8.0)	8.0 (6.0–10.0)	8.8 (7.3–10.5)	0.29	7.5 (6.0–9.0)	9.0 (7.0–10.0)	0.17
MRAP, mmHg	7.0 (5.0–8.0)	7.0 (5.0–9.0)	7.0 (5.0–8.0)	5.5 (5.0–7.5)	0.35	7.0 (5.0–7.0)	6.0 (5.0–8.0)	0.96
RVEDP, mmHg	8.0 (6.0–10.0)	9.0 (6.0–11.0)	8.6 (7.0–10.2)	7.0 (5.1–8.6)	0.05	9.0 (7.0–9.9)	7.0 (6.0–9.1)	0.18
CI, L/min/m <sup>2</sup>	3.38 (2.98–3.82)	3.52 (3.23–3.98)	3.23 (2.94–3.98)	3.42 (3.00–3.68)	0.93	3.23 (3.03–3.63)	3.38 (2.84–3.82)	0.95
Qp/Qs	1.00 (1.00–1.00)	1.00 (0.93–1.00)	1.00 (1.00–1.19)	1.00 (1.00–1.00)	0.09	1.16 (1.00–1.55)†	1.00 (1.00–1.00)	0.0043*
PVRI, WU·m <sup>2</sup>	6.79 (4.10–10.89)	15.8 (11.7–19.1)	7.64 (4.81–13.89)	5.33 (3.48–6.96)	0.07	7.67 (5.57–14.09)	5.60 (3.21–8.70)	0.08
PVR/SVR	0.37 (0.25–0.60)	0.85 (0.77–1.12)	0.49 (0.23–0.69)	0.33 (0.25–0.38)	0.22	0.49 (0.26–0.77)	0.34 (0.25–0.53)	0.29

CHD and shunt *P* values represent comparison between those without/with CHD and a shunt, respectively. Data are presented as n (%) or median (interquartile range). CHD indicates congenital heart disease; CI, cardiac index; DPAP, diastolic pulmonary arterial pressure; DTPG, diastolic transpulmonary gradient; MAP, mean (systemic) arterial pressure; MLAP, mean left atrial pressure or pulmonary capillary wedge pressure; MPAP, mean pulmonary arterial pressure; MRAP, mean right atrial pressure; PH, pulmonary hypertension; PVRI, indexed pulmonary vascular resistance; Qp/Qs, ratio of pulmonary-to-systemic blood flow; RVEDP, right ventricular end-diastolic pressure; SPAP, systolic pulmonary arterial pressure; SVR, systemic vascular resistance; and TPG, mean transpulmonary gradient.

\**P*<0.05.

†Four patients had a net right-to-left shunt (Qp:Qs of 0.94, 0.86, 0.89, and 0.93).

3 quartiles (*P*<0.0001 for both). Echocardiographic measures for this quartile are compared with their matched controls in Table 3. These patients demonstrated worsened diastolic dysfunction: further reduced pulmonary vein S and D, mitral *E*, *E'*, and septal *E'* and further increased mitral *E* deceleration time, isovolumic relaxation time, eccentricity indices, and RV systolic prolongation. Apical recoil remained increased (more negative), as did indexed diastolic untwist rate.

#### Congenital Heart Disease

We further analyzed PH patients by presence of CHD. Those with CHD demonstrated increased pulmonary vein A velocity (0.17 [0.14–0.21] versus 0.14 [0.10–0.18] m/s; *P*=0.0382) and decreased septal *E'* (8.0 [7.0–10.0] versus 10.0 [8.0–13.0] cm/s; *P*=0.0344), compared with those without CHD (respectively). There were no other statistically significant differences in diastolic measures or RV systolic duration (*P*>0.05 for all).

#### Shunting

We further analyzed PH patients by presence of a shunt. There were no statistically significant differences in LV diastolic measures or RV systolic duration between those with and those without a shunt (*P*>0.05 for all).

#### Relationships With LV Diastolic Measures

##### Invasive Hemodynamics

Invasive hemodynamics are related to LV echocardiographic diastolic measures shown in Table 4. Positive moderate correlations were seen with LV isovolumic relaxation time and weak correlations with *E* deceleration time. Negative moderate and weak correlations were seen with mitral *E*, *E/A*, *E'/A'*, septal

*E'*, DLSR, and mid and apical DCSR. Pulmonary venous measures did not correlate with invasive hemodynamics (*P*>0.05 for all). LV *E/E'* did not correlate with MPAP/MAP, PVRI, or left atrial pressure/PCWP (*r*=0.13; *P*=0.36). Similarly, invasively measured left atrial pressure/PCWP did not correlate with predicted PCWP using Nagueh original regression formula, when using either the lateral mitral *E'* alone (*r*=0.09; *P*=0.51) or a combined average of lateral mitral *E'* and septal *E'* in the equation (*r*=0.2; *P*=0.15).<sup>20</sup>

##### Septal Shift

Eccentricity index is related to LV echocardiographic diastolic measures shown in Table 5. Systolic and diastolic eccentricity index demonstrated moderate and weak positive correlations with pulmonary A duration, *E* deceleration time, isovolumic relaxation time, and *E/E'* and moderate and weak negative correlations with pulmonary vein S and D, mitral *E'*, septal *E'*, *A'*, DLSR, basal and mid DCSR, and apical recoil. Additionally, weak negative correlations were seen between systolic eccentricity index with mitral *E* and *E'/A'* and diastolic eccentricity index with mitral *A'*.

##### Prolonged RV Systole

Prolonged RV systole, which was strongly associated with MPAP/MAP (*r*=0.71; *P*<0.0001) and PVRI (*r*=0.70; *P*<0.0001), is related to echocardiographic LV diastolic measures shown in Table 5. Prolonged RV systole demonstrated moderate and weak negative correlations with pulmonary vein S and D, mitral *E*, *E/A*, *E'*, *E'/A'*, and septal *E'* and weak positive correlations with pulmonary vein A duration, *E* deceleration time, and isovolumic relaxation.

Table 3. LV Echocardiographic Variables

	Control Subjects (n=53)	PH Patients (n=53)	P Value	Severe PH (n=13)	P Value
2-dimensional measures					
End-diastolic eccentricity index	1.02 (0.96 to 1.06)	1.18 (1.09 to 1.28)	<0.0001*	1.43 (1.15 to 1.76)	0.043*
End-systolic eccentricity index	0.99 (0.96 to 1.03)	1.27 (1.11 to 1.50)	<0.0001*	1.82 (1.30 to 2.17)	0.005*
End-diastolic volume, mL	49.0 (29.0 to 79.5)	52.0 (26.0 to 90.0)	0.25	77.0 (39.0 to 105.0)	0.75
Indexed end-diastolic volume, mL/m <sup>2</sup>	37.9 (32.8 to 48.4)	44.3 (37.2 to 59.8)	0.07	61.5 (45.6 to 82.4)	0.61
End-systolic volume, mL	16.5 (9.5 to 27.5)	19.0 (12.0 to 46.0)	0.004*	33.0 (16.0 to 47.0)	0.46
Indexed end-systolic volume, mL/m <sup>2</sup>	12.9 (9.8 to 16.5)	20.3 (14.2 to 28.1)	0.0006*	23.5 (21.4 to 33.1)	0.24
Biplane ejection fraction, %	66.0 (62.0 to 69.0)	56.0 (50.0 to 63.0)	<0.0001*	58.0 (50.0 to 66.0)	0.015*
Doppler measures					
Pulmonary vein					
S, m/s	0.46 (0.38 to 0.49)	0.31 (0.27 to 0.37)	<0.0001*	0.28 (0.20 to 0.34)	0.0063*
D, m/s	0.60 (0.53 to 0.67)	0.46 (0.40 to 0.55)	<0.0001*	0.42 (0.40 to 0.47)	0.045*
S/D ratio	0.75 (0.65 to 0.86)	0.71 (0.56 to 0.83)	0.22	0.62 (0.57 to 0.83)	0.25
A, m/s	0.16 (0.13 to 0.18)	0.15 (0.12 to 0.19)	0.84	0.16 (0.13 to 0.19)	0.89
A duration, ms	68.0 (59.0 to 83.0)	85.0 (69.0 to 107.0)	<0.0001*	91.0 (70.0 to 107.0)	0.12
Mitral valve					
E, m/s	0.96 (0.85 to 1.10)	0.86 (0.73 to 0.93)	0.011*	0.74 (0.71 to 0.82)	0.035*
A, m/s	0.47 (0.39 to 0.57)	0.49 (0.34 to 0.72)	0.12	0.49 (0.39 to 0.62)	0.14
E/A	1.99 (1.66 to 2.54)	1.80 (1.16 to 2.87)	0.53	1.54 (1.08 to 2.04)	0.12
E deceleration time, ms	133.0 (121.0 to 170.0)	179.0 (137.0 to 210.0)	0.0002*	222.5 (153.5 to 279.5)	0.032*
Inflow duration, ms	400.5 (306.5 to 579.0)	363.0 (263.0 to 497.5)	0.013*	416.0 (304.5 to 497.5)	0.37
PVAD/MVAD	0.65 (0.57 to 0.79)	0.72 (0.62 to 0.84)	0.017*	0.70 (0.67 to 0.78)	0.18
PVAD–MVAD	–38.0 (–48.0 to –20.0)	–29.5 (–45.0 to –14.0)	0.09	–30.0 (–45.0 to –20.0)	0.31
RV/LV systolic duration	1.01 (0.98 to 1.032)	1.12 (1.06 to 1.18)	<0.0001*	1.19 (1.14 to 1.30)	0.0005*
Tissue Doppler imaging					
Lateral mitral E', cm/s	18.8 (16.0 to 20.2)	12.0 (9.0 to 15.0)	<0.0001*	10.0 (8.5 to 13.0)	0.027*
Lateral mitral A', cm/s	6.4 (5.4 to 7.9)	6.0 (4.0 to 7.0)	0.15	6.0 (4.0 to 7.0)	0.03*
Lateral mitral E'/A'	2.9 (2.3 to 3.3)	2.1 (1.7 to 3.0)	0.001*	1.9 (1.7 to 2.5)	0.16
Septal E', cm/s	14.5 (13.0 to 16.0)	9.0 (7.0 to 11.0)	<0.0001*	7.0 (6.0 to 9.0)	0.0003*
Septal A', cm/s	6.3 (5.9 to 7.0)	5.0 (4.0 to 6.0)	0.0002*	5.0 (3.5 to 6.0)	0.0303*
Isovolumic relaxation time, ms	47.0 (38.0 to 52.0)	58.0 (48.0 to 72.0)	0.0003*	76.5 (56.5 to 98.5)	0.009*
Mitral valve E/E'	5.2 (4.5 to 6.0)	7.2 (6.0 to 9.5)	<0.0001*	7.3 (6.0 to 8.9)	0.033*
Speckle-tracking echocardiography					
Global DLSR, 1/s	2.17 (1.84 to 2.68)	2.08 (1.53 to 2.45)	0.05	1.55 (1.26 to 2.08)	0.05
Basal global DCSR, 1/s	2.05 (1.54 to 2.78)	1.44 (1.20 to 2.48)	0.019*	1.19 (1.13 to 1.68)	0.023*
Mid global DCSR, 1/s	1.78 (1.42 to 2.10)	1.68 (1.23 to 1.99)	0.06	1.22 (1.09 to 1.74)	0.17
Apical global DCSR, 1/s	2.48 (1.73 to 2.79)	2.34 (1.67 to 2.85)	0.88	1.85 (1.29 to 2.52)	0.44
Apical recoil, %/s	–49.8 (–18.9 to –75.5)	–80.9 (–49.2 to –107.2)	0.0009*	–72.6 (–52.5 to –95.5)	0.0008*
Basal recoil, %/s	39.4 (18.1 to 54.1)	16.4 (7.3 to 41.2)	0.70	15.9 (–3.3 to 38.3)	0.17
Indexed diastolic untwist rate, %/s/cm	–11.3 (–7.8 to –16.4)	–15.4 (–11.5 to –22.4)	0.003*	–14.9 (–8.3 to –15.4)	0.0162*

Data are presented as median (interquartile range). Severe PH patients are compared with their matched controls (not shown). A indicates pulmonary vein flow during atrial contraction; A, late transmitral flow velocity; A', peak late diastolic myocardial annular velocity; D, diastolic pulmonary vein flow; DCSR, diastolic circumferential strain rate; DLSR, diastolic longitudinal strain rate; E, early transmitral flow velocity; E', peak early diastolic myocardial annular velocity; LV, left ventricle; MVAD, mitral valve A duration; PH, pulmonary hypertension; PVAD, pulmonary vein A duration; RV, right ventricle; and S, systolic pulmonary vein flow.

\* $P < 0.05$ .

**Table 4. Correlations Between Left Ventricular Diastolic Measures and Invasive Hemodynamics**

Left Ventricular Diastolic Variable	MPAP/MAP		PVRi		DPAP		TPG		DTPG	
	<i>r</i>	<i>P</i> Value								
Mitral valve										
<i>E</i>	−0.35	0.0125*	−0.52	<0.0001*	−0.36	0.0098*	−0.42	0.0017*	−0.39	0.0046*
<i>A</i>	0.26	0.08	0.10	0.50	0.22	0.12	0.22	0.12	0.25	0.08
<i>E/A</i>	−0.37	0.0115*	−0.35	0.0138*	−0.36	0.0129*	−0.40	0.0037*	−0.41	0.0036*
<i>E</i> deceleration time	0.14	0.34	0.30	0.0284*	0.26	0.07	0.20	0.16	0.24	0.10
Inflow duration	−0.09	0.56	0.07	0.64	−0.03	0.86	−0.04	0.77	−0.06	0.68
Tissue Doppler imaging										
Lateral mitral <i>E'</i>	−0.16	0.29	−0.18	0.22	−0.11	0.45	−0.14	0.34	−0.09	0.54
Lateral mitral <i>A'</i>	0.19	0.19	0.17	0.25	0.29	0.0394*	0.22	0.12	0.30	0.0354*
Lateral mitral <i>E'/A'</i>	−0.31	0.0314*	−0.27	0.056	−0.29	0.0429*	−0.27	0.056	−0.29	0.0431*
Septal <i>E'</i>	−0.49	0.0002*	−0.50	0.0001*	−0.47	0.0004*	−0.49	0.0002*	−0.47	0.0004*
Septal <i>A'</i>	0.04	0.81	0.02	0.90	0.08	0.59	0.05	0.71	0.11	0.44
Isovolumic relaxation time	0.45	0.0013*	0.58	<0.0001*	0.46	0.0007*	0.47	0.0003*	0.48	0.0004*
Mitral valve <i>E/E'</i>	−0.01	0.95	−0.10	0.47	−0.07	0.64	−0.08	0.57	−0.10	0.51
Speckle-tracking echocardiography										
Global DLSR	−0.37	0.0097*	−0.50	0.0002*	−0.42	0.0024*	−0.40	0.0034*	−0.44	0.0016*
Basal global DCSR	−0.22	0.16	−0.27	0.07	−0.21	0.16	−0.23	0.13	−0.18	0.26
Mid global DCSR	−0.21	0.15	−0.36	0.0107*	−0.24	0.10	−0.26	0.07	−0.26	0.08
Apical global DCSR	−0.23	0.14	−0.38	0.0066*	−0.25	0.09	−0.31	0.0332*	−0.27	0.07
Apical recoil	0.08	0.61	0.11	0.50	0.08	0.64	0.03	0.83	0.07	0.66
Basal recoil	−0.05	0.77	0.04	0.82	0.04	0.83	−0.03	0.84	0.003	0.98
Indexed diastolic untwist rate	0.16	0.16	0.22	0.16	0.14	0.40	0.14	0.39	0.15	0.37

*A* indicates late transmitral flow velocity; *A'*, peak late diastolic myocardial annular velocity; DCSR, diastolic circumferential strain rate; DLSR, diastolic longitudinal strain rate; DPAP, diastolic pulmonary artery pressure; DTPG, diastolic transpulmonary gradient; *E*, early transmitral flow velocity; *E'*, peak early diastolic myocardial annular velocity; MPAP/MAP, mean pulmonary-to-systemic arterial pressure ratio; PVRi, indexed pulmonary vascular resistance; and TPG, mean transpulmonary gradient.

\**P*<0.05.

### Reproducibility

Intraobserver intraclass correlation coefficients (95% confidence interval) were LV DLSR=0.88 (0.73–0.95), basal DCSR=0.73 (0.44–0.88), mid DCSR=0.86 (0.70–0.94), and apical DCSR=0.92 (0.81–0.97). Interobserver intraclass correlation coefficients (95% confidence interval) were LV DLSR=0.92 (0.82–0.97), basal DCSR=0.69 (0.44–0.84), mid DCSR=0.78 (0.59–0.89), and apical DCSR=0.68 (0.42–0.84).

### Discussion

Using simultaneous echocardiography and catheterization, we evaluated LV diastolic function in pediatric PH and the relation to invasive hemodynamics, septal shift, and prolonged RV systole. The main findings of this study are the following: (1) children with PH have LV early diastolic dysfunction in a pattern most consistent with impaired relaxation, although features of reduced ventricular compliance are also present; (2) tissue Doppler and strain imaging data suggest myocardial dysfunction beyond changes in LV filling patterns; and (3) LV diastolic dysfunction is associated with the severity of invasive hemodynamics, leftward septal shift, and prolonged RV systole. Although we cannot directly relate our findings to

mortality because of low event rate, the findings are important for several reasons. First, whereas the overwhelming majority of studies emphasize RV systolic dysfunction in PH, this is one of the first to highlight LV diastolic dysfunction in pediatric PH—certainly with simultaneous cardiopulmonary hemodynamics. Second, because invasive hemodynamics determine outcomes, the correlation with LV diastolic parameters is likely important. Third, in many cardiovascular conditions, diastolic dysfunction is a significant determinant of outcomes.<sup>21</sup> Last, biventricular dysfunction likely confers worse outcomes.<sup>22</sup>

### LV Diastolic Measures

Although systolic measures like LV ejection fraction and cardiac index were within normal ranges (even in severe PH), pediatric PH patients demonstrate LV diastolic dysfunction by multiple indices. The pattern is most consistent with impaired relaxation, with progressively reduced early diastolic filling and prolonged isovolumic relaxation and *E* deceleration times as PH worsens—a pattern also seen in adult PH.<sup>7–9,23–27</sup>

Abnormal LV filling in PH is thought to arise predominantly from 2 causes: (1) diminished RV output because of

**Table 5. Correlations Between Left Ventricular Diastolic Measures, Septal Shift, and Prolonged Right Ventricular Systole**

Left Ventricular Diastolic Variable	End-Systolic Eccentricity Index		End-Diastolic Eccentricity Index		Prolonged Right Ventricular Systole	
	<i>r</i>	<i>P</i> Value	<i>r</i>	<i>P</i> Value	<i>R</i>	<i>P</i> Value
<b>Pulmonary vein</b>						
S	-0.46	<0.0001*	-0.49	<0.0001*	-0.47	<0.0001*
D	-0.37	0.0004*	-0.30	0.0056*	-0.33	0.0012*
S/D ratio	-0.09	0.42	-0.14	0.20	-0.10	0.37
A	0.06	0.59	0.03	0.77	0.10	0.37
A duration	0.40	0.0004*	0.33	0.0042*	0.32	0.0053*
<b>Mitral valve</b>						
<i>E</i>	-0.24	0.0266*	-0.17	0.13	-0.36	0.0002*
<i>A</i>	0.09	0.43	-0.04	0.70	0.13	0.20
<i>E/A</i>	-0.15	0.17	0.001	0.99	-0.23	0.0308*
<i>E</i> deceleration time	0.34	0.0014*	0.38	0.0002*	0.32	0.0018*
<b>Tissue Doppler imaging</b>						
Lateral mitral <i>E'</i>	-0.45	<0.0001*	-0.35	0.0010*	-0.42	<0.0001*
Lateral mitral <i>A'</i>	-0.18	0.10	-0.25	0.0229*	-0.05	0.67
Lateral mitral <i>E'/A'</i>	-0.22	0.0494*	-0.12	0.29	-0.37	0.0002*
Septal <i>E'</i>	-0.58	<0.0001*	-0.45	<0.0001*	-0.55	<0.0001*
Septal <i>A'</i>	-0.30	0.0061*	-0.31	0.0039*	-0.18	0.07
Isovolumic relaxation time	0.44	<0.0001*	0.35	0.0008*	0.36	0.0008*
Mitral valve <i>E/E'</i>	0.34	0.0017*	0.29	0.0080*	0.27	0.0086*
<b>Speckle-tracking echocardiography</b>						
Global DLSR	-0.32	0.0027*	-0.30	0.0052*	-0.14	0.24
Basal global DCSR	-0.35	0.0011*	-0.43	<0.0001*	-0.20	0.08
Mid global DCSR	-0.22	0.0369*	-0.23	0.0314*	-0.07	0.53
Apical global DCSR	-0.11	0.34	-0.16	0.13	-0.13	0.26
Apical recoil	-0.24	0.0327*	-0.21	0.07	-0.33	0.0056*
Basal recoil	-0.18	0.11	-0.10	0.40	-0.12	0.32
Indexed diastolic untwist rate	-0.13	0.27	-0.14	0.22	-0.29	0.0133*

A indicates pulmonary vein flow during atrial contraction; *A*, late transmitral flow velocity; *A'*, peak late diastolic myocardial annular velocity; *D*, diastolic pulmonary vein flow; DCSR, diastolic circumferential strain rate; DLSR, diastolic longitudinal strain rate; *E*, early transmitral flow velocity; *E'*, peak early diastolic myocardial annular velocity; and *S*, systolic pulmonary vein flow.

\**P*<0.05.

increased afterload, resulting in reduced LV preload (series effect) and (2) leftward septal shift directly interfering with LV filling (direct effect). Baker et al<sup>28</sup> elegantly demonstrated that the 2 causes are inter-related and both responsible for impaired LV filling. Prolonged RV systolic duration, which causes leftward septal shift, inefficient RV contraction, and reduced RV filling time, likely worsens both mechanisms.

Although early filling and relaxation abnormalities predominated, increased pulmonary venous *A* duration in relation to mitral *A* duration and mitral *E/E'* suggest decreased LV compliance. We intentionally selected patients with normal left-sided filling pressures to avoid confounding LV adaptations in PH, so changes consistent with reduced compliance may precede an occult rise in end-diastolic pressure. LV

fibrosis seen in animals with RV hypertension,<sup>29</sup> and possibly in adults with PH,<sup>30</sup> likely affects ventricular relaxation and compliance. Thus, as in pediatric cardiomyopathy, our data suggest that there can be a mixed picture of early diastolic dysfunction/impaired relaxation and decreased compliance in pediatric PH.<sup>31</sup> Notably, similar to tricuspid *E/E'* and RV end-diastolic pressure, mitral *E/E'* may not accurately reflect LV filling pressures in pediatric PH.<sup>32</sup>

PH patients demonstrated diastolic myocardial dysfunction, beyond altered filling patterns alone, with free-wall and septal tissue Doppler changes and reduced early diastolic strain rate. Progressively increased isovolumic relaxation time in PH corroborates impaired LV relaxation before mitral valve opening. Similar diastolic myocardial alterations have been found

in adult PH by echocardiography and recently by cardiac magnetic resonance imaging, with some relation to outcomes.<sup>33,34</sup>

Although our PH patients were younger with less chronic/severe PH than published adult populations, numerous parameters of LV diastolic dysfunction were already present. It is unclear whether such changes are reversible or improve with improving RV function during therapy and thus warrant further investigation. Notably, no patient demonstrated systemic hypoxemia, which alone can impair ventricular function.

Temporal disparities between RV and LV contraction and relaxation also impact diastolic function in PH. We previously found that RV systolic duration increases at the expense of diastole with increasing PH severity—quantified by the systolic-to-diastolic ratio.<sup>35</sup> Here, RV systole was prolonged in PH, by a measure that included isovolumic relaxation for a few reasons. First, there may be postsystolic myocardial shortening after pulmonary valve closure that does not contribute to RV ejection but may disrupt LV early diastolic function.<sup>11</sup> Second, in PH patients, RV pressure during isovolumic relaxation may be higher than LV pressure (which may be in isovolumic relaxation or mitral inflow) and may still exert septal shift and direct diastolic interaction. Magnetic resonance imaging studies demonstrate prolonged RV systole in PH, corresponding with leftward septal shift and impaired LV filling<sup>11</sup> and that peak LV filling rate occurs after maximal septal bowing.<sup>7</sup> That mitral inflow may begin while the RV is still in isovolumic relaxation with elevated pressures, or even before the completion of RV systole, highlights the confusion in easily defining systole and diastole in PH, which may occur at different times for each ventricle. This likely contributes to adverse ventricular–ventricular interactions.

Not all changes observed were consistent with reduced diastolic function. Apical recoil was increased in PH, enough to overcome reduced basal recoil and yield an increase in the diastolic untwist rate. Apical diastolic myocardial mechanics may potentially compensate for reduced basal mechanics or altered diastolic filling in PH.

#### **CHD and Shunts**

The presence of CHD or a shunt did not greatly alter echocardiographic LV diastolic measures. In contrast, we previously found different RV diastolic perturbations based on the presence of a shunt.<sup>32</sup> In any event, the presence of a shunt in PH remains clinically relevant.<sup>36–38</sup>

#### **Relationships With LV Diastolic Measures**

Numerous, albeit modest, correlations between invasive hemodynamics and echocardiographic LV diastolic measures support progressive diastolic dysfunction with worsening PH hemodynamics and highlight the relationship between pulmonary impedance and LV filling. Similarly, leftward septal shift and prolonged RV systole were related to most measures of impaired LV relaxation, demonstrating pathological early diastolic ventricular–ventricular interactions. We found similar modest correlations between RV diastolic measures and cardiopulmonary hemodynamics,<sup>32</sup> where diastolic dysfunction has clear clinical implications.<sup>2–4</sup> Collectively, these suggest that worsening PH hemodynamics, with increased leftward septal shift and prolonged RV systole, all contribute to LV early diastolic dysfunction, which may ultimately impact outcomes.

#### **Limitations**

The cross-sectional nature of this study and the low number of deaths precluded analysis of the prognostic significance of the diastolic parameters investigated. The heterogeneity of our study population (PH cause, CHD, active shunts) may limit our ability to detect consistent diastolic changes but accurately reflects the pediatric PH population. Selection bias could have been introduced because some controls presented to a cardiologist for evaluation, or that PH patients presented to a tertiary care center, although hemodynamic data suggest a mixture of well-controlled and poorly controlled PH. We chose to stratify PH severity by MPAP/MAP, given this reflects the degree of PH in pediatrics better than other pressure measures alone. However, other invasive measures could have been used to stratify patients as well. Because of the large number of comparisons and correlations performed on a modest number of patients, the possibility of type I error exists.

The altered measures presented likely reflect pathological ventricular interdependence, related in part to geometric changes, but may not represent intrinsic LV dysfunction. However, as it would have incurred unnecessary risk to patients, the LV was not accessed during the clinically indicated right-heart catheterization and so the relatively load-independent measure tau and invasive measures of LV compliance were not assessed. Over-/underwedged PCWP can affect estimation of left atrial pressure, although PCWP is standard of care to estimate mean left atrial pressure during right-heart catheterization, and we preferentially used left atrial pressures when obtained. We attempted to have consistent catheterization protocols between both sites, and although fluid-filled catheters were used at both locations, SickKids used Millar catheters for RV pressure assessment. Oxygen consumption was measured by mass spectrometry at SickKids and estimated by the LaFarge table at Children's Hospital Colorado, although this does not affect pressure measurements. We used institutionally matched controls given altitude differences between Denver and Toronto, which can affect PVRi and MPAP. PH patients were all under general anesthesia, although we did not dictate an anesthesia regimen or duration, or the timing of catheterization during anesthesia. Subtle differences in anesthetics and ventilation could affect hemodynamics and thus potentially diastolic measures, possibly limiting comparisons with unsedated controls; it would not limit comparisons between diastolic measures and hemodynamics.

#### **Conclusions**

Pediatric PH patients exhibit LV diastolic dysfunction most consistent with impaired relaxation with reduced myocardial deformation, related to invasive hemodynamics, leftward septal shift, and prolonged RV systole. Although focus is placed on RV systolic dysfunction in PH, our results highlight that pediatric PH involves biventricular systolic and diastolic dysfunction, which should stimulate further research into the importance of adverse ventricular interdependence and LV diastolic dysfunction in pediatric PH.

#### **Sources of Funding**

This research was supported in part by The Frederick and Margaret L. Weyerhaeuser Foundation, The Jayden de Luca Foundation,

the Canadian Institutes of Health Research, and NIH grants R01HL114753, U01HL121518, and UL1TR000154.

## Disclosures

None.

## References

- D'Alonzo GE, Barst RJ, Ayres SM, Bergofsky EH, Brundage BH, Detre KM, Fishman AP, Goldring RM, Groves BM, Kernis JT. Survival in patients with primary pulmonary hypertension. Results from a national prospective registry. *Ann Intern Med.* 1991;115:343–349.
- Voelkel NF, Quaife RA, Leinwand LA, Barst RJ, McGoon MD, Meldrum DR, Dupuis J, Long CS, Rubin LJ, Smart FW, Suzuki YJ, Gladwin M, Denholm EM, Gail DB; National Heart, Lung, and Blood Institute Working Group on Cellular and Molecular Mechanisms of Right Heart Failure. Right ventricular function and failure: report of a National Heart, Lung, and Blood Institute working group on cellular and molecular mechanisms of right heart failure. *Circulation.* 2006;114:1883–1891. doi: 10.1161/CIRCULATIONAHA.106.632208.
- Chin KM, Kim NH, Rubin LJ. The right ventricle in pulmonary hypertension. *Coron Artery Dis.* 2005;16:13–18.
- Bogaard HJ, Abe K, Vonk Noordegraaf A, Voelkel NF. The right ventricle under pressure: cellular and molecular mechanisms of right-heart failure in pulmonary hypertension. *Chest.* 2009;135:794–804. doi: 10.1378/chest.08-0492.
- Hardegree EL, Sachdev A, Fenstad ER, Villarraga HR, Frantz RP, McGoon MD, Oh JK, Ammash NM, Connolly HM, Eidem BW, Pellikka PA, Kane GC. Impaired left ventricular mechanics in pulmonary arterial hypertension: identification of a cohort at high risk. *Circ Heart Fail.* 2013;6:748–755. doi: 10.1161/CIRCHEARTFAILURE.112.000098.
- Burkett DA, Slorach C, Patel SS, Redington AN, Ivy DD, Mertens L, Younoszai AK, Friedberg MK. Left ventricular myocardial function in children with pulmonary hypertension: relation to right ventricular performance and hemodynamics. *Circ Cardiovasc Imaging.* 2015;8:e003260. doi: 10.1161/CIRCIMAGING.115.003260.
- Gan C, Lankhaar JW, Marcus JT, Westerhof N, Marques KM, Bronzwaer JG, Boonstra A, Postmus PE, Vonk-Noordegraaf A. Impaired left ventricular filling due to right-to-left ventricular interaction in patients with pulmonary arterial hypertension. *Am J Physiol Heart Circ Physiol.* 2006;290:H1528–H1533. doi: 10.1152/ajpheart.01031.2005.
- Louie EK, Rich S, Brundage BH. Doppler echocardiographic assessment of impaired left ventricular filling in patients with right ventricular pressure overload due to primary pulmonary hypertension. *J Am Coll Cardiol.* 1986;8:1298–1306.
- Moustapha A, Kaushik V, Diaz S, Kang SH, Barasch E. Echocardiographic evaluation of left-ventricular diastolic function in patients with chronic pulmonary hypertension. *Cardiology.* 2001;95:96–100.
- Tonelli AR, Plana JC, Heresi GA, Dweik RA. Prevalence and prognostic value of left ventricular diastolic dysfunction in idiopathic and heritable pulmonary arterial hypertension. *Chest.* 2012;141:1457–1465. doi: 10.1378/chest.11-1903.
- Marcus JT, Gan CT, Zwanenburg JJ, Boonstra A, Allaart CP, Götte MJ, Vonk-Noordegraaf A. Interventricular mechanical asynchrony in pulmonary arterial hypertension: left-to-right delay in peak shortening is related to right ventricular overload and left ventricular underfilling. *J Am Coll Cardiol.* 2008;51:750–757. doi: 10.1016/j.jacc.2007.10.041.
- Vonk-Noordegraaf A, Marcus JT, Gan CT, Boonstra A, Postmus PE. Interventricular mechanical asynchrony due to right ventricular pressure overload in pulmonary hypertension plays an important role in impaired left ventricular filling. *Chest.* 2005;128(suppl 6):628S–630S. doi: 10.1378/chest.128.6\_suppl.628S.
- Marcus JT, Vonk Noordegraaf A, Roeleveld RJ, Postmus PE, Heethaar RM, Van Rossum AC, Boonstra A. Impaired left ventricular filling due to right ventricular pressure overload in primary pulmonary hypertension: noninvasive monitoring using MRI. *Chest.* 2001;119:1761–1765.
- Stojnic BB, Brecker SJ, Xiao HB, Helmy SM, Mbaissourom M, Gibson DG. Left ventricular filling characteristics in pulmonary hypertension: a new mode of ventricular interaction. *Br Heart J.* 1992;68:16–20.
- Galiè N, Hoepfer MM, Humbert M, Torbicki A, Vachiery JL, Barbera JA, Beghetti M, Corris P, Gaine S, Gibbs JS, Gomez-Sanchez MA, Jondeau G, Klepetko W, Opitz C, Peacock A, Rubin L, Zellweger M, Simonneau G; ESC Committee for Practice Guidelines (CPG). Guidelines for the diagnosis and treatment of pulmonary hypertension: the Task Force for the Diagnosis and Treatment of Pulmonary Hypertension of the European Society of Cardiology (ESC) and the European Respiratory Society (ERS), endorsed by the International Society of Heart and Lung Transplantation (ISHLT). *Eur Heart J.* 2009;30:2493–2537. doi: 10.1093/eurheartj/ehp297.
- Lai WW, Geva T, Shirali GS, Frommelt PC, Humes RA, Brook MM, Pignatelli RH, Rychik J; Task Force of the Pediatric Council of the American Society of Echocardiography; Pediatric Council of the American Society of Echocardiography. Guidelines and standards for performance of a pediatric echocardiogram: a report from the Task Force of the Pediatric Council of the American Society of Echocardiography. *J Am Soc Echocardiogr.* 2006;19:1413–1430. doi: 10.1016/j.echo.2006.09.001.
- Ryan T, Petrovic O, Dillon JC, Feigenbaum H, Conley MJ, Armstrong WF. An echocardiographic index for separation of right ventricular volume and pressure overload. *J Am Coll Cardiol.* 1985;5:918–927.
- Voigt JU, Pedrizzetti G, Lysyansky P, Marwick TH, Houle H, Baumann R, Pedri S, Ito Y, Abe Y, Metz S, Song JH, Hamilton J, Sengupta PP, Kolias TJ, d'Hooge J, Aurigemma GP, Thomas JD, Badano LP. Definitions for a common standard for 2D speckle tracking echocardiography: consensus document of the EACVI/ASE/Industry Task Force to standardize deformation imaging. *Eur Heart J Cardiovasc Imaging.* 2015;16:1–11. doi: 10.1093/ehjci/jeu184.
- Biner S, Rafique AM, Ray I, Cuk O, Siegel RJ, Tolstrup K. Aortopathy is prevalent in relatives of bicuspid aortic valve patients. *J Am Coll Cardiol.* 2009;53:2288–2295. doi: 10.1016/j.jacc.2009.03.027.
- Nagueh SF, Middleton KJ, Kopelen HA, Zoghbi WA, Quiñones MA. Doppler tissue imaging: a noninvasive technique for evaluation of left ventricular relaxation and estimation of filling pressures. *J Am Coll Cardiol.* 1997;30:1527–1533.
- McMahon CJ, Nagueh SF, Pignatelli RH, Denfield SW, Dreyer WJ, Price JF, Clunie S, Bezold LI, Hays AL, Towbin JA, Eidem BW. Characterization of left ventricular diastolic function by tissue Doppler imaging and clinical status in children with hypertrophic cardiomyopathy. *Circulation.* 2004;109:1756–1762. doi: 10.1161/01.CIR.0000124723.16433.31.
- Le Tourneau T, Deswarte G, Lambin N, Foucher-Hossein C, Fayad G, Richardson M, Polge AS, Vannesson C, Topilsky Y, Juthier F, Trochu JN, Enriquez-Sarano M, Bauters C. Right ventricular systolic function in organic mitral regurgitation: impact of biventricular impairment. *Circulation.* 2013;127:1597–1608. doi: 10.1161/CIRCULATIONAHA.112.000999.
- Mahmud E, Raisinghani A, Hassankhani A, Sadeghi HM, Strachan GM, Auger W, DeMaria AN, Blanchard DG. Correlation of left ventricular diastolic filling characteristics with right ventricular overload and pulmonary artery pressure in chronic thromboembolic pulmonary hypertension. *J Am Coll Cardiol.* 2002;40:318–324.
- Gurudevan SV, Malouf PJ, Auger WR, Waltman TJ, Madani M, Raisinghani AB, DeMaria AN, Blanchard DG. Abnormal left ventricular diastolic filling in chronic thromboembolic pulmonary hypertension: true diastolic dysfunction or left ventricular underfilling? *J Am Coll Cardiol.* 2007;49:1334–1339. doi: 10.1016/j.jacc.2007.01.028.
- Dittrich HC, Chow LC, Nicod PH. Early improvement in left ventricular diastolic function after relief of chronic right ventricular pressure overload. *Circulation.* 1989;80:823–830.
- Menzel T, Wagner S, Kramm T, Mohr-Kahaly S, Mayer E, Braeuninger S, Meyer J. Pathophysiology of impaired right and left ventricular function in chronic embolic pulmonary hypertension: changes after pulmonary thromboendarterectomy. *Chest.* 2000;118:897–903.
- Boussuges A, Pinet C, Molenat F, Burnet H, Ambrosi P, Badier M, Sainy JM, Orehek J. Left atrial and ventricular filling in chronic obstructive pulmonary disease. An echocardiographic and Doppler study. *Am J Respir Crit Care Med.* 2000;162(2 pt 1):670–675. doi: 10.1164/ajrccm.162.2.9908056.
- Baker AE, Dani R, Smith ER, Tyberg JV, Belenkie I. Quantitative assessment of independent contributions of pericardium and septum to direct ventricular interaction. *Am J Physiol.* 1998;275(2 pt 2):H476–H483.
- Friedberg MK, Cho MY, Li J, Assad RS, Sun M, Rohailla S, Honjo O, Apitz C, Redington AN. Adverse biventricular remodeling in isolated right ventricular hypertension is mediated by increased transforming growth factor- $\beta$ 1 signaling and is abrogated by angiotensin receptor blockade. *Am J Respir Cell Mol Biol.* 2013;49:1019–1028. doi: 10.1165/rcmb.2013-0149OC.
- Manders E, Bogaard HJ, Handoko ML, van de Veerdonk MC, Keogh A, Westerhof N, Stienen GJ, Dos Remedios CG, Humbert M, Dorfmueller P, Fadel E, Guignabert C, van der Velden J, Vonk-Noordegraaf A, de Man FS, Ottenheijm CA. Contractile dysfunction of left ventricular cardiomyocytes in patients with pulmonary arterial hypertension. *J Am Coll Cardiol.* 2014;64:28–37. doi: 10.1016/j.jacc.2014.04.031.

31. Dragulescu A, Mertens L, Friedberg MK. Interpretation of left ventricular diastolic dysfunction in children with cardiomyopathy by echocardiography: problems and limitations. *Circ Cardiovasc Imaging*. 2013;6:254–261. doi: 10.1161/CIRCIMAGING.112.000175.
32. Okumura K, Slorach C, Mroczek D, Dragulescu A, Mertens L, Redington AN, Friedberg MK. Right ventricular diastolic performance in children with pulmonary arterial hypertension associated with congenital heart disease: correlation of echocardiographic parameters with invasive reference standards by high-fidelity micromanometer catheter. *Circ Cardiovasc Imaging*. 2014;7:491–501. doi: 10.1161/CIRCIMAGING.113.001071.
33. Huez S, Vachiéry JL, Unger P, Brimiouille S, Naeije R. Tissue Doppler imaging evaluation of cardiac adaptation to severe pulmonary hypertension. *Am J Cardiol*. 2007;100:1473–1478. doi: 10.1016/j.amjcard.2007.06.047.
34. Knight DS, Steeden JA, Moledina S, Jones A, Coghlan JG, Muthurangu V. Left ventricular diastolic dysfunction in pulmonary hypertension predicts functional capacity and clinical worsening: a tissue phase mapping study. *J Cardiovasc Magn Reson*. 2015;17:116. doi: 10.1186/s12968-015-0220-3.
35. Alkon J, Humpl T, Manlhiot C, McCrindle BW, Reyes JT, Friedberg MK. Usefulness of the right ventricular systolic to diastolic duration ratio to predict functional capacity and survival in children with pulmonary arterial hypertension. *Am J Cardiol*. 2010;106:430–436. doi: 10.1016/j.amjcard.2010.03.048.
36. Barst RJ, Ivy DD, Foreman AJ, McGoon MD, Rosenzweig EB. Four- and seven-year outcomes of patients with congenital heart disease-associated pulmonary arterial hypertension (from the REVEAL Registry). *Am J Cardiol*. 2014;113:147–155. doi: 10.1016/j.amjcard.2013.09.032.
37. Bui MT, Grollmus O, Ly M, Mandache A, Fadel E, Decante B, Serraf A. Surgical palliation of primary pulmonary arterial hypertension by a unidirectional valved Potts anastomosis in an animal model. *J Thorac Cardiovasc Surg*. 2011;142:1223–1228. doi: 10.1016/j.jtcvs.2010.10.060.
38. Baruteau AE, Serraf A, Lévy M, Petit J, Bonnet D, Jais X, Vouhé P, Simonneau G, Belli E, Humbert M. Potts shunt in children with idiopathic pulmonary arterial hypertension: long-term results. *Ann Thorac Surg*. 2012;94:817–824. doi: 10.1016/j.athoracsur.2012.03.099.

### CLINICAL PERSPECTIVE

We evaluated left ventricular diastolic function in children and young adults with pulmonary hypertension by echocardiography, performed simultaneously with cardiac catheterization to allow direct comparisons between invasive hemodynamics and echocardiographic measures. We included unique, previously understudied pulmonary hypertension populations, including pediatric patients, those with congenital heart disease, and those with intra/extracardiac shunts. We documented left ventricular diastolic dysfunction in a pattern most consistent with impaired relaxation, although some aspects of reduced ventricular compliance were also present. Changes were more pronounced in those with severe pulmonary hypertension. Beyond changes in left ventricular filling patterns, tissue Doppler and diastolic strain imaging data suggest left ventricular myocardial dysfunction in pulmonary hypertension. There were minimal differences in diastolic measures between those with and without congenital heart disease or between those with and without a shunt. Echocardiographic measures of diastolic function were associated with invasive hemodynamics, as well as leftward septal shift and prolonged right ventricular systole, which likely play an important role in left ventricular diastolic dysfunction in pulmonary hypertension. Although much focus is placed on right ventricular systolic dysfunction in pulmonary hypertension, our results show that through ventricular interdependence, pediatric pulmonary hypertension patients have evidence of left ventricular diastolic dysfunction. Future research is needed to determine the clinical importance of left ventricular diastolic dysfunction in this population and the reversibility of such changes.

## Impact of Pulmonary Hemodynamics and Ventricular Interdependence on Left Ventricular Diastolic Function in Children With Pulmonary Hypertension

Dale A. Burkett, Cameron Slorach, Sonali S. Patel, Andrew N. Redington, D. Dunbar Ivy, Luc Mertens, Adel K. Younoszai and Mark K. Friedberg

*Circ Cardiovasc Imaging*. 2016;9:

doi: 10.1161/CIRCIMAGING.116.004612

*Circulation: Cardiovascular Imaging* is published by the American Heart Association, 7272 Greenville Avenue, Dallas, TX 75231

Copyright © 2016 American Heart Association, Inc. All rights reserved.

Print ISSN: 1941-9651. Online ISSN: 1942-0080

The online version of this article, along with updated information and services, is located on the World Wide Web at:

<http://circimaging.ahajournals.org/content/9/9/e004612>

**Permissions:** Requests for permissions to reproduce figures, tables, or portions of articles originally published in *Circulation: Cardiovascular Imaging* can be obtained via RightsLink, a service of the Copyright Clearance Center, not the Editorial Office. Once the online version of the published article for which permission is being requested is located, click Request Permissions in the middle column of the Web page under Services. Further information about this process is available in the [Permissions and Rights Question and Answer](#) document.

**Reprints:** Information about reprints can be found online at:  
<http://www.lww.com/reprints>

**Subscriptions:** Information about subscribing to *Circulation: Cardiovascular Imaging* is online at:  
<http://circimaging.ahajournals.org/subscriptions/>